



Hard X-ray Imaging by Solar Orbiter STIX: the MEM_GE method

Paolo Massa

Department of Physics and Astronomy, Western Kentucky University

Joint work with: Volpara A., Battaglia A. F., Perracchione E., Garbarino S.,
Benvenuto F., Massone A. M., Hurford G. J., Krucker S., Piana M. & the
STIX team

December 7, 2022, Max Plank Institute for Radio Astronomy

WKU

Outline

- The STIX imaging concept
- The MEM_GE method
- Results
- Data calibration

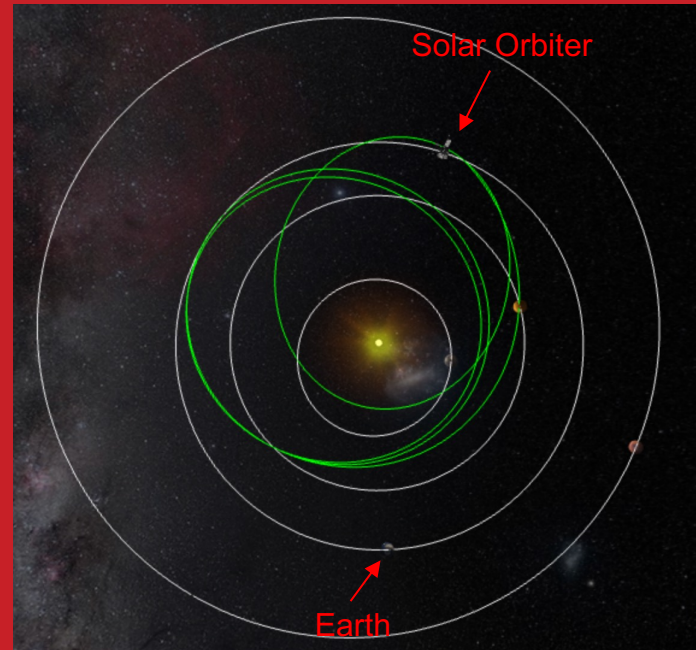
The STIX imaging concept

STIX in Solar Orbiter



credits: ESA website

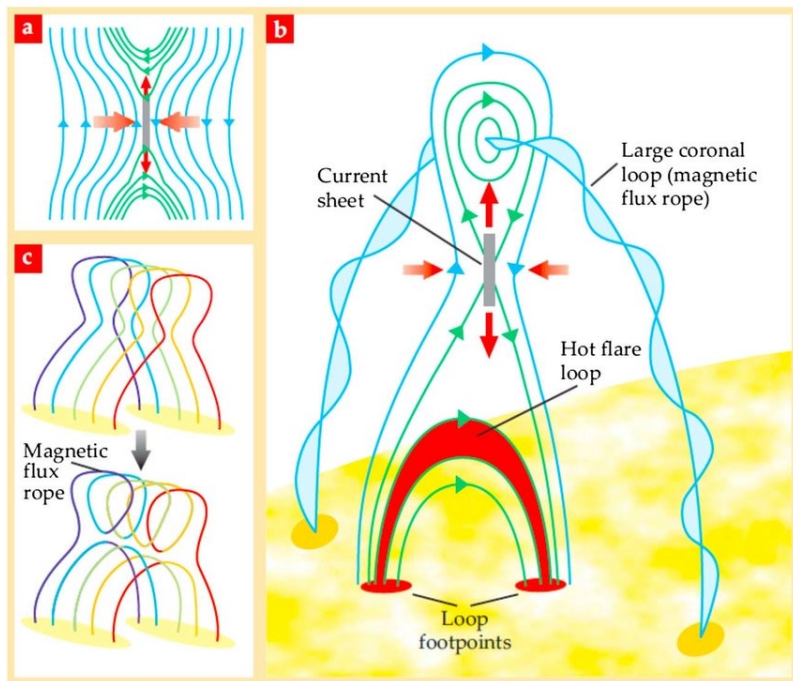
Solar Orbiter trajectory



<https://solarorbiter.esac.esa.int/where/>

WKU®

The STIX instrument



STIX: Spectrometer/Telescope for Imaging X-rays

Scientific goal: provide information on electrons accelerated during a solar flare and on the plasma temperature

How: by measuring X-ray photons emitted by bremsstrahlung

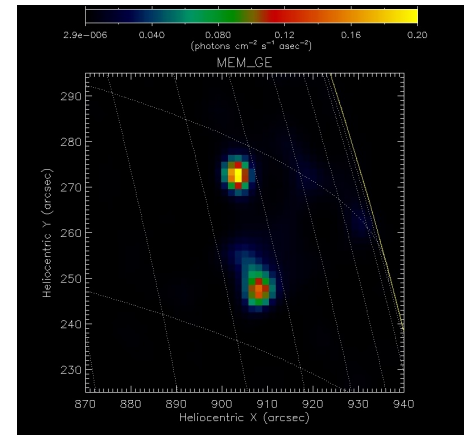
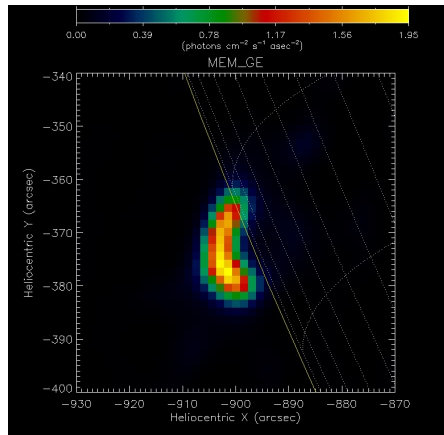
The STIX instrument

STIX imaging objective:

reconstruct the image of the flaring X-ray emission from indirect measurements

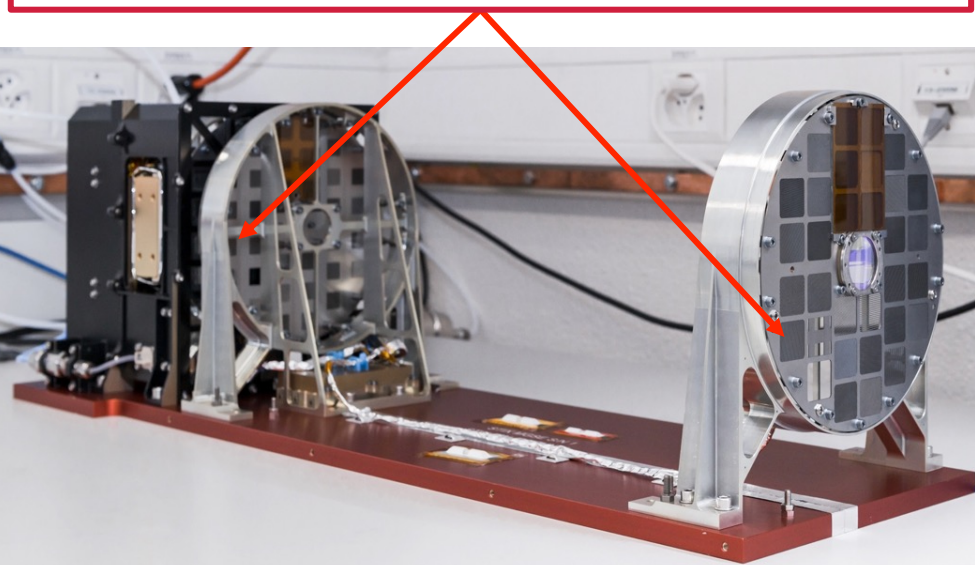
Fourier components of the angular distribution of the X-ray source

Examples from RHESSI data (Lin et al., 2002)



The STIX instrument

Subcollimator = front grid + rear grid + detector

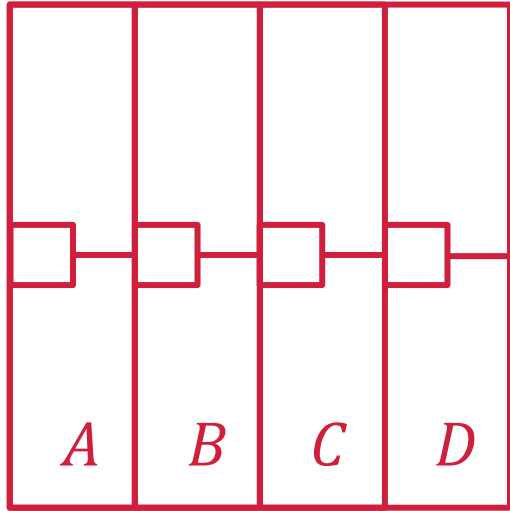


Bigrid imaging system

STIX consists of 32 subcollimators:

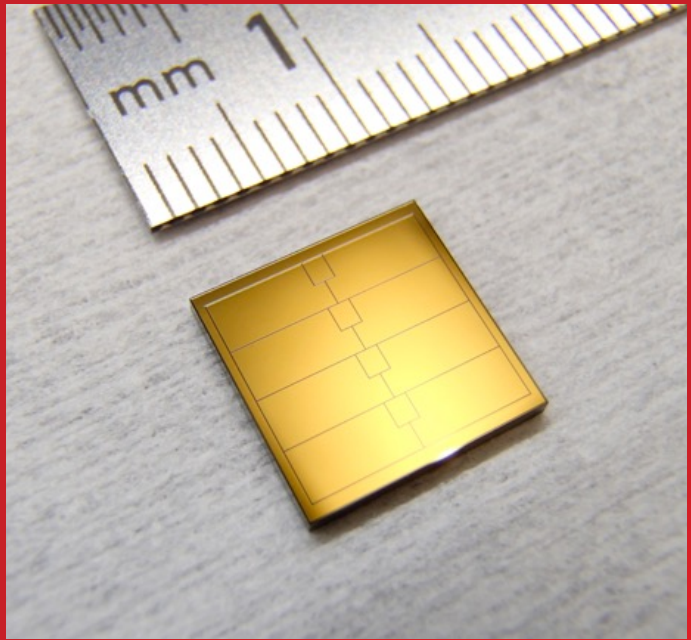
- 30 are used for imaging
- Coarse Flare Locator
- Background monitor

The STIX instrument



A, B, C and D: number of counts recorded by the detector pixels

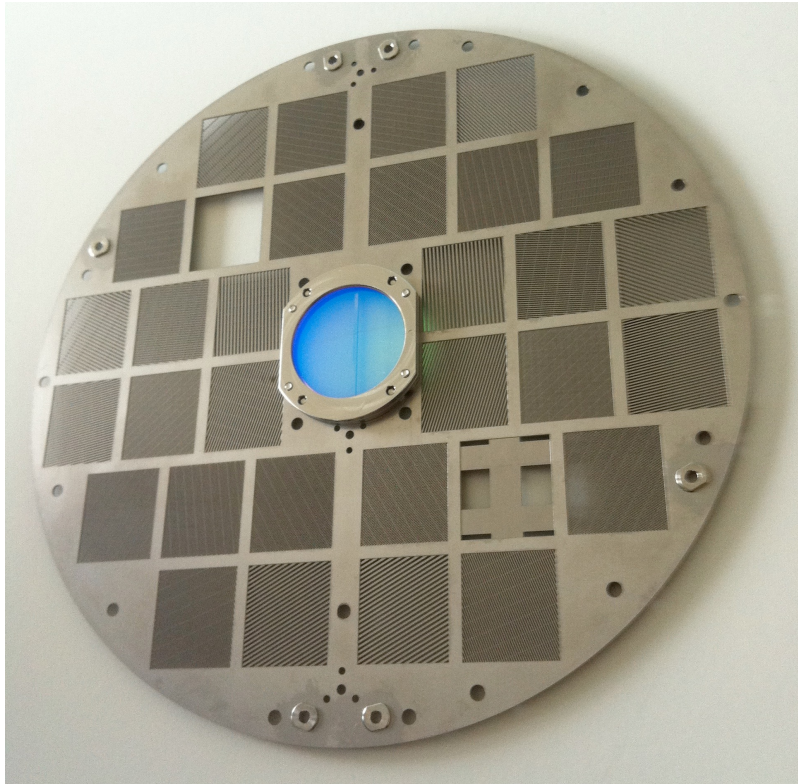
STIX Cadmium-Telluride detector
(Meuris et al. 2015)



Krucker et al., 2020

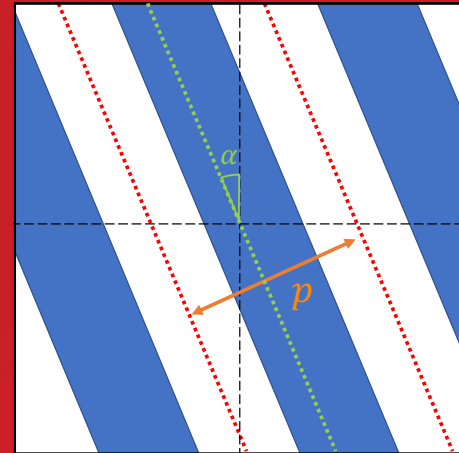
WKU

The STIX instrument



Grid parameters:

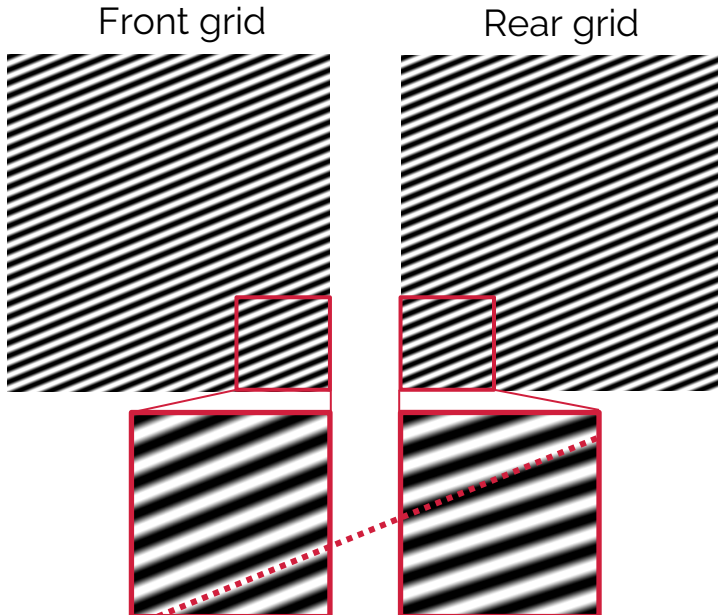
- α : orientation angle
- p : pitch = distance between two consecutive slit centers



WKU®

The STIX imaging concept

Front and rear grid have different orientation and pitch

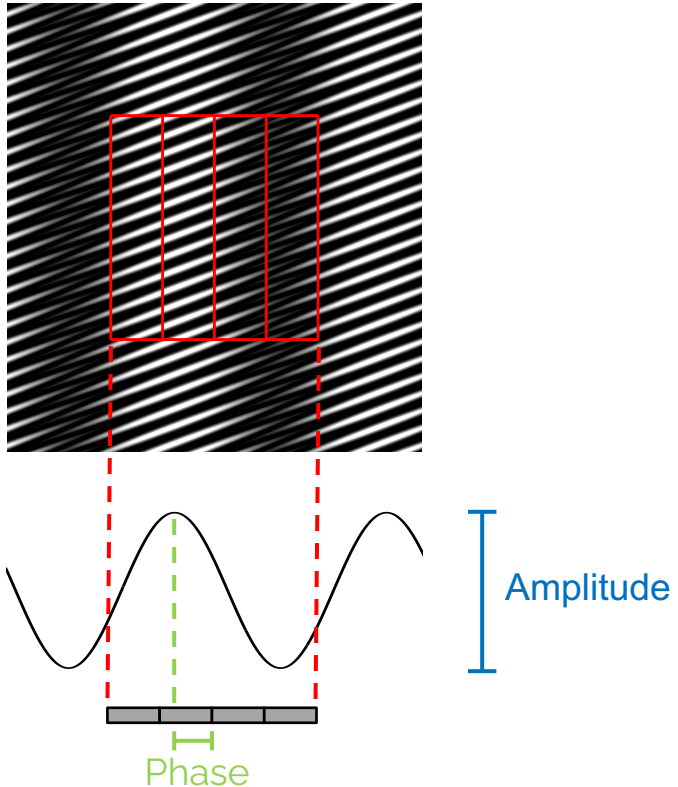


The transmitted X-ray photon flux creates a **Moiré pattern**



WKU

The STIX imaging concept

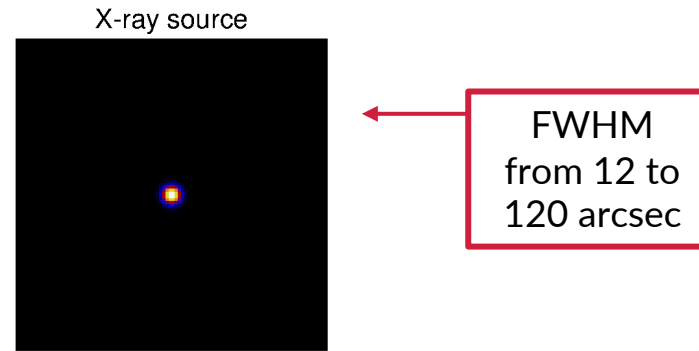


Moiré patterns have:

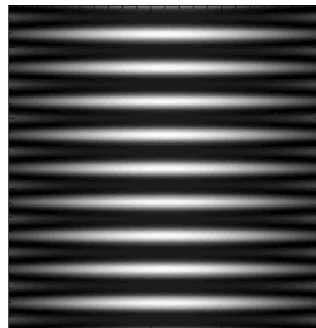
- period equal to the detector width
- orientation perpendicular to the pixels stripes
- amplitude sensitive to the size of the X-ray source
- phase sensitive to the X-ray source location

The STIX imaging concept

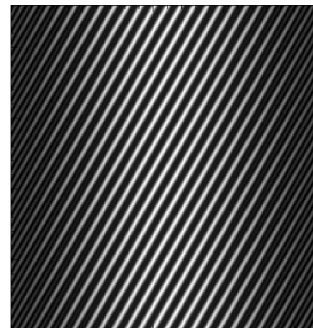
The amplitude of a Moiré pattern is sensitive to the source size



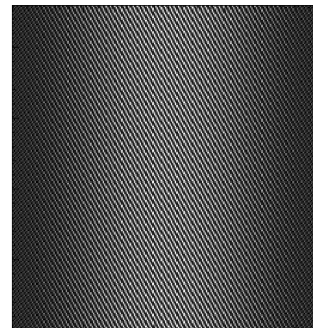
Resolution: 178.6 arcsec



Resolution: 61.0 arcsec

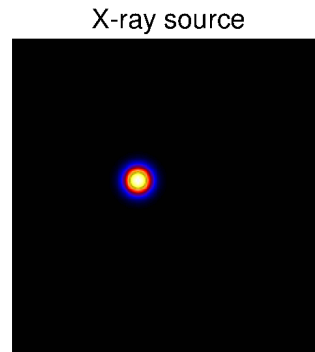


Resolution: 20.9 arcsec

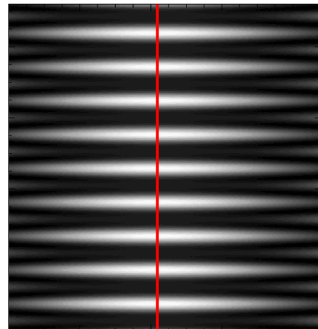


The STIX imaging concept

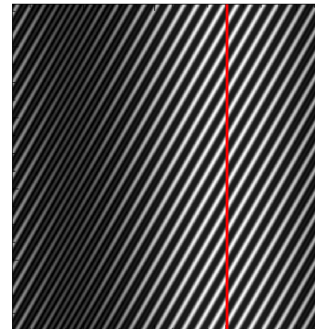
The phase of a Moiré pattern is sensitive to the source location



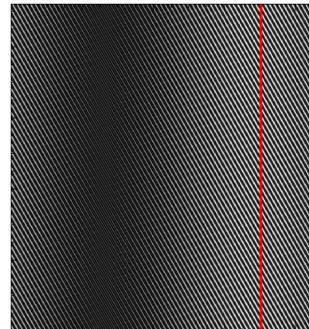
Resolution: 178.6 arcsec



Resolution: 61.0 arcsec



Resolution: 20.9 arcsec



The STIX imaging concept

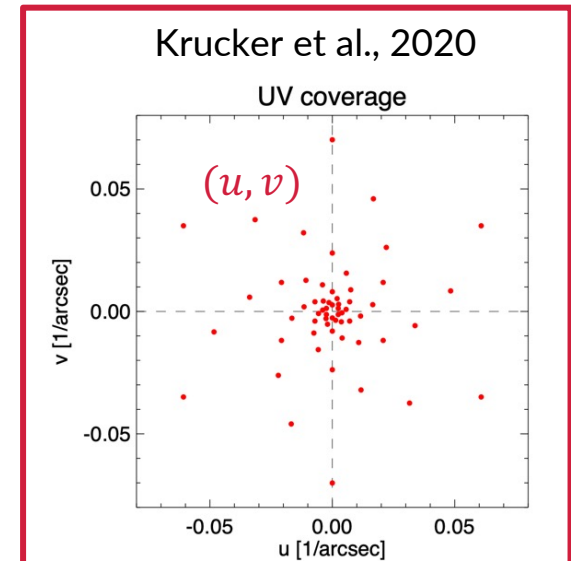
$\phi(x, y)$ represents the intensity of the X-ray radiation emitted from (x, y) on the Sun disk

Data measured by STIX: $\mathbf{V} = (V_1, \dots, V_{30})$, where

$$V = \iint \phi(x, y) \exp(2\pi i(xu + yv)) dx dy$$

- $|V| \propto \sqrt{(C - A)^2 + (D - B)^2}$
- $\phi = \text{atan}\left(\frac{D-B}{C-A}\right) + 45^\circ + \phi_{\text{calib}}$

Determined by count measurements



Determined by grids' pitch and orientation

The STIX imaging concept

$\phi(x, y)$ represents the intensity of the X-ray radiation emitted from (x, y) on the Sun disk

Data measured by STIX: $\mathbf{V} = (V_1, \dots, V_{30})$, where

$$V = \iint \phi(x, y) \exp(2\pi i(xu + yv)) dx dy$$

Image reconstruction problem for STIX: determine ϕ s.t.

$$\mathbf{F}\phi = \mathbf{V}$$

where \mathbf{F} is the Fourier transform computed in the STIX frequencies

MEM_GE

(Massa et al., 2020)

The MEM_GE optimization problem

The MEM_GE optimization problem is the one of determining

$$\phi^* = \operatorname{argmin}_{\phi} \chi^2(\phi) + \lambda H(\phi)$$

subject to: $\phi \geq 0$, $\sum_i \phi_i = \Phi$

where:

$$1. \chi^2(\phi) = \left\| \frac{\mathcal{F}\phi - V}{\sigma} \right\|^2$$

$$2. H(\phi) = - \sum_i \phi_i \log \left(\frac{\phi_i}{c} \right)$$

3. $\lambda > 0$ is the regularization parameter

Balance between data fitting
and “smoothness” of the
solution

MEM_GE (Massa et al. (2020))

The MEM_GE optimization problem can be rewritten as

$$\phi^* = \operatorname{argmin}_{\phi} \left\| \frac{\mathcal{F}\phi - V}{\sigma} \right\|^2 + \lambda H(\phi) + \delta_P(\phi) + \delta_F(\phi)$$

where

$$\delta_P(\phi) = \begin{cases} 0, & \phi \geq 0 \\ +\infty, & \text{else} \end{cases} \quad \delta_F(\phi) = \begin{cases} 0, & \sum_i \phi_i = \Phi \\ +\infty, & \text{else} \end{cases}$$

Defined $f(\phi) = \left\| \frac{\mathcal{F}\phi - V}{\sigma} \right\|^2$ and $g(\phi) = \lambda H(\phi) + \delta_P(\phi) + \delta_F(\phi)$ we have the following

Lemma 1:

- i. f is differentiable with Lipschitz continuous gradient (and Lipschitz constant L)
- ii. f and g are convex, proper, lower semicontinuous
- iii. $f + g$ is coercive

MEM_GE (Massa et al. (2020))

Lemma 2 (Combettes & Pesquet (2011)):

- i. The MEM_GE optimization problem admits unique solution
- ii. The iterative scheme

$$\phi_{k+1} = \text{prox}_{\eta_k g}(\phi_k - \eta_k \nabla f(\phi_k)), \\ k \in \mathbb{N}$$

converges to the solution if we choose
 $\eta_k < \frac{2}{L}$ for all $k \in \mathbb{N}$.

Definition: Given $h: \mathbb{R}^M \rightarrow \mathbb{R} \cup \{+\infty\}$ a proper, lower semicontinuous and convex function, we define

$$\text{prox}_h(x) = \arg \min_{y \in \mathbb{R}^M} \frac{1}{2} \|x - y\|^2 + h(y)$$

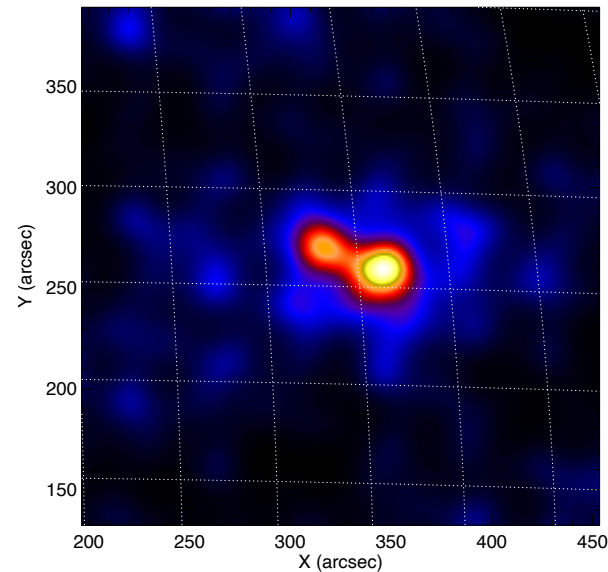
MEM_GE algorithm with FISTA acceleration (Beck & Teboulle (2009))

```
Fix  $\Phi_0 \in \mathbb{R}^N$  ( $\Phi_0 \geq 0$ ),  $z_0 = \Phi_0$ ,  $t_0 = 1$  and  $\varepsilon > 0$ ;  
for  $k = 0$  to  $k_{max} - 1$  do  
   $p_k = \text{prox}_{\frac{1}{L}g}(z_k - \frac{1}{L}\nabla \chi^2(z_k));$   
  if  $(\chi^2 + g)(p_k) \leq (\chi^2 + g)(\Phi_k)$  then  
     $\Phi_{k+1} = p_k;$   
    if  $\|\Phi_{k+1} - \Phi_k\| < \varepsilon \|\Phi_k\|$  then  
      break;  
    end  
  else  
     $\Phi_{k+1} = \Phi_k;$   
  end  
   $t_{k+1} = \frac{1 + \sqrt{1 + 4t_k^2}}{2};$   
   $\tau_k = \frac{t_k - 1}{t_{k+1}};$   
   $z_{k+1} = \Phi_{k+1} + \tau_k(\Phi_{k+1} - \Phi_k) + \frac{t_k}{t_{k+1}}(p_k - \Phi_{k+1});$   
end
```

MEM_GE (Massa et al. (2020))

How does the solution depend on λ ?

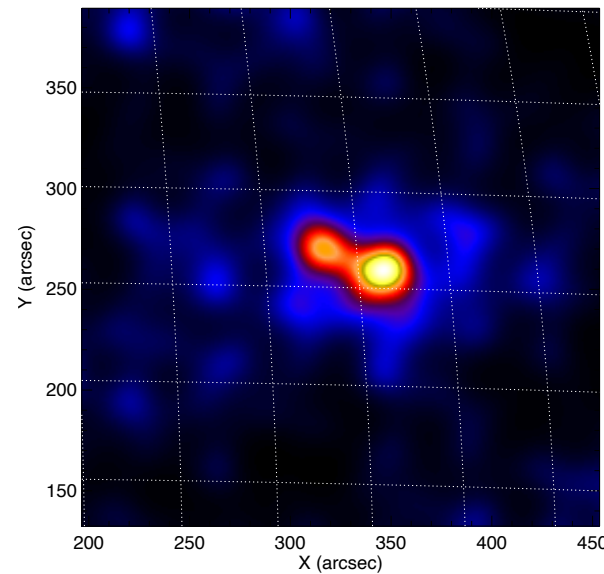
Large λ



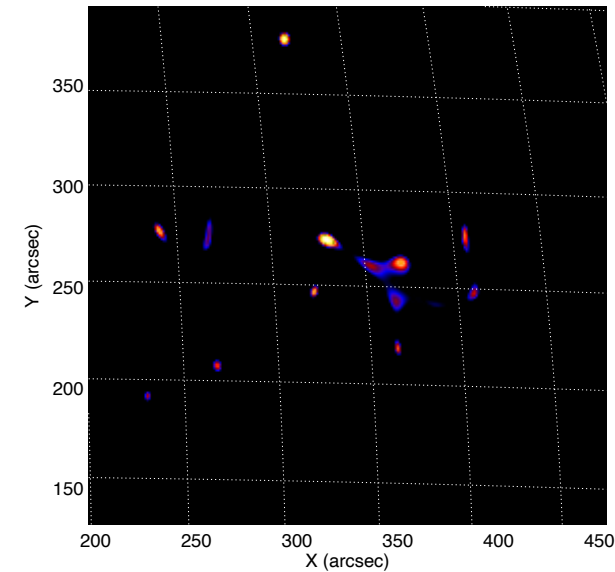
MEM_GE (Massa et al. (2020))

How does the solution depend on λ ?

Large λ



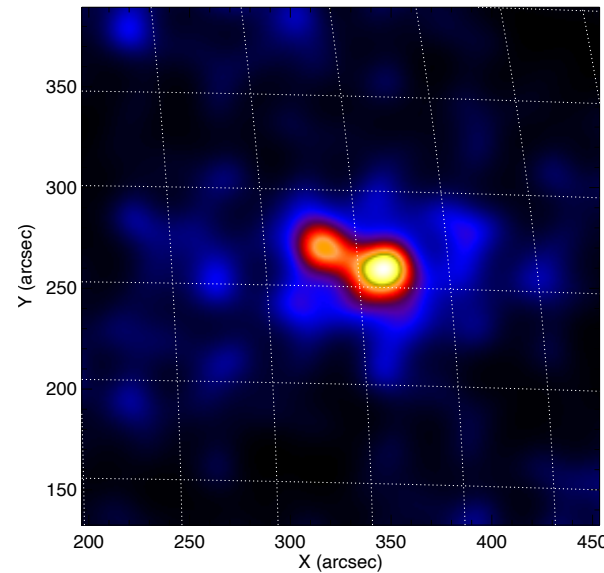
Low λ



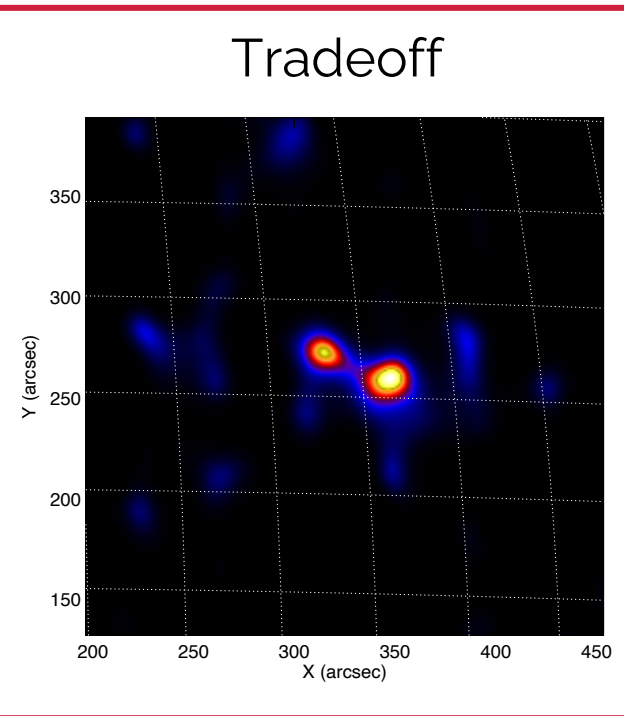
MEM_GE (Massa et al. (2020))

How does the solution depend on λ ?

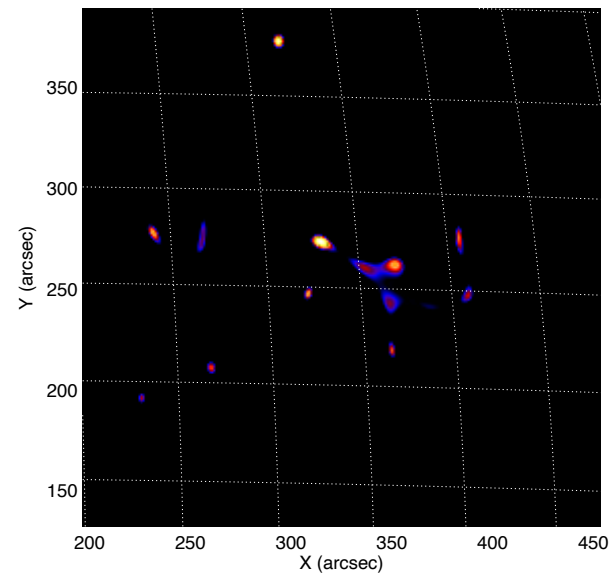
Large λ



Tradeoff

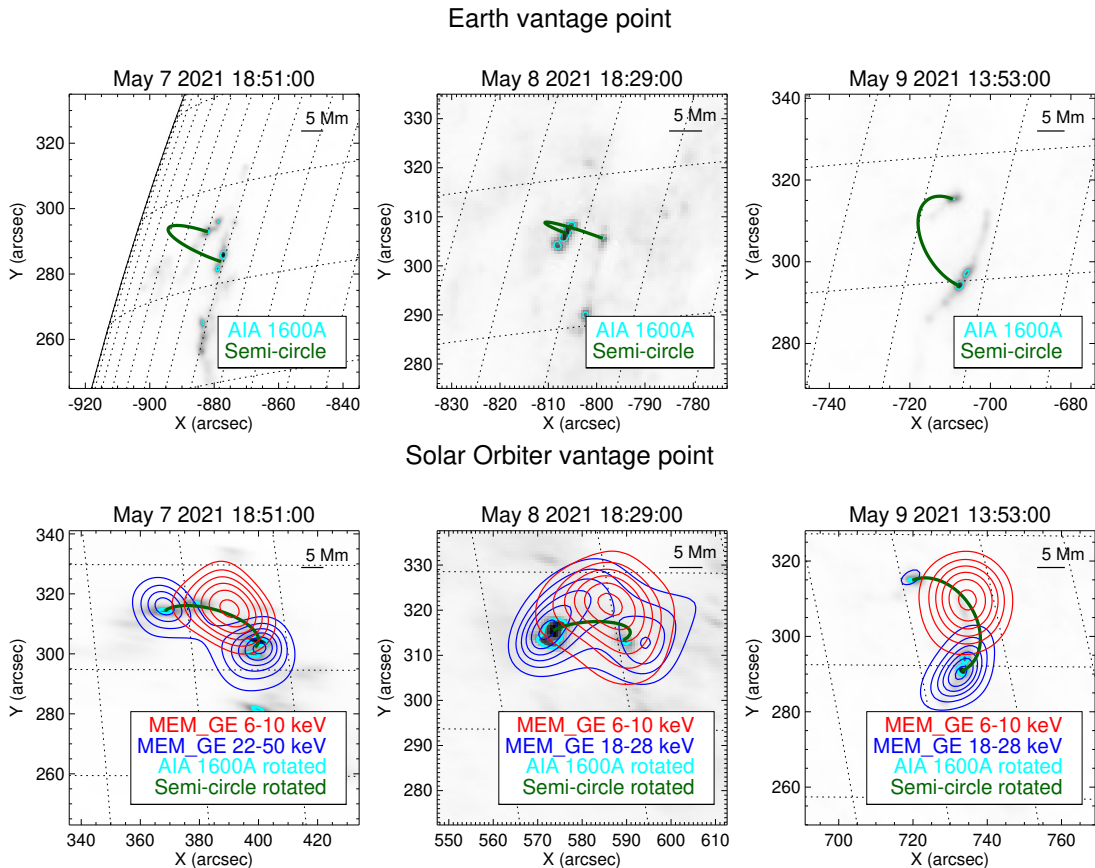


Low λ



Results

First imaging results (Massa et al., 2022)



Active region AR2822

- May 7: GOES M3.9
- May 8: GOES C8.6
- May 9: GOES C4.0

Manual shift STIX reconstructions

Event	Δx (arcsec)	Δy (arcsec)
May 7	44	54
May 8	45	57
May 9	47.5	53

Data calibration

Data redundancy

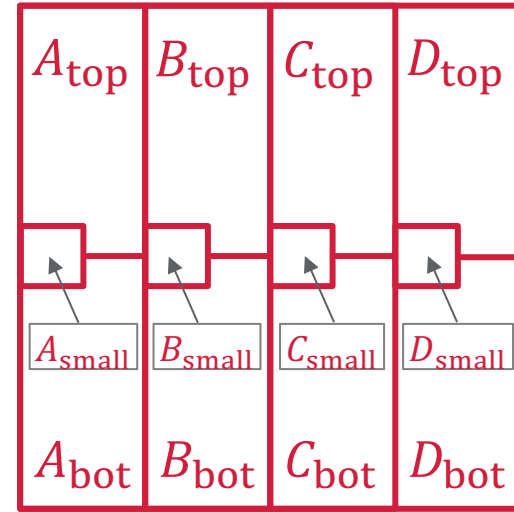
In each sub-collimator:

- $A_{\text{top}}, B_{\text{top}}, C_{\text{top}}, D_{\text{top}}$ must be equal to $A_{\text{bot}}, B_{\text{bot}}, C_{\text{bot}}, D_{\text{bot}}$ and to $A_{\text{small}}, B_{\text{small}}, C_{\text{small}}, D_{\text{small}}$
- $A + C = B + D$ for each row of pixels (or combinations of them), independently from the source morphology

An estimate of the total flux of the X-ray source is given by

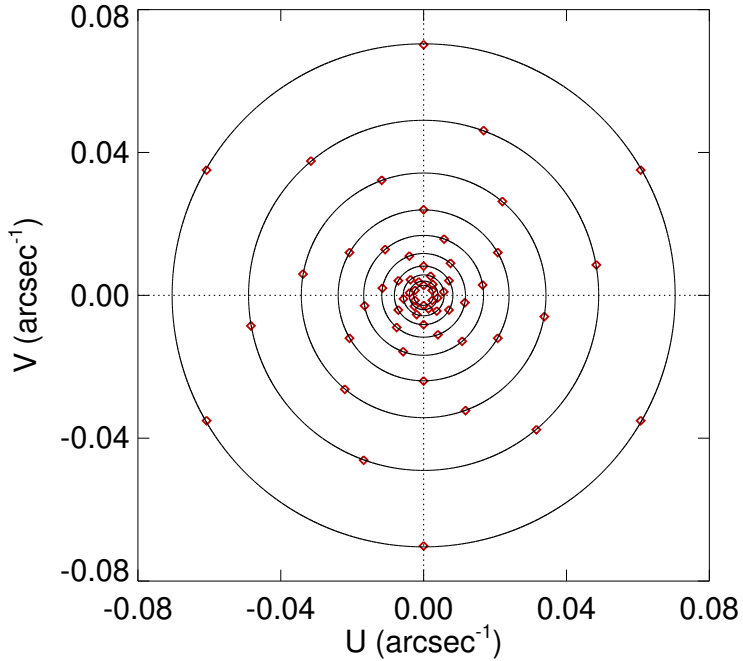
$$A + C + B + D$$

which should be equal for every detector



Data redundancy

- STIX samples 10 different resolutions from 7.1 and 179 arcsec, logarithmically spaced in steps of 1.43
- For each resolution 3 different detectors sample the as many orientations



Closure phase definition (valid for point sources):

A signed sum of the 3 phases of the visibilities measured by the sub-collimators with the same resolution is equal to 0 modulo 2π

Back-projection lines

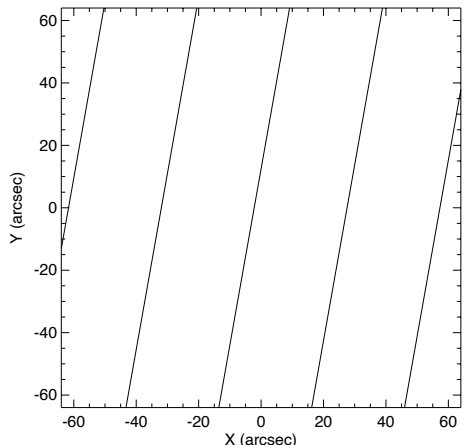
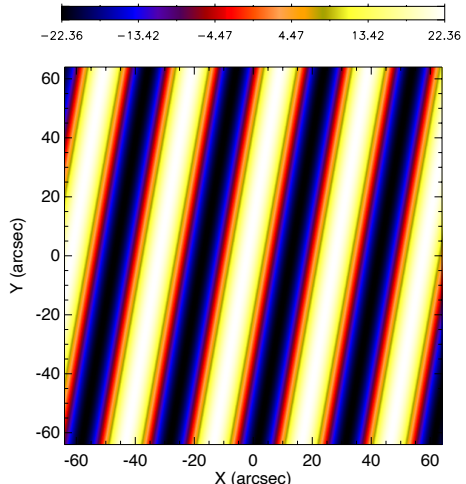
- The back-projection of a single visibility is a sinusoidal wave defined by

$$\phi(x, y) = \mathcal{A} \cos(2\pi(xu + yv) - \omega)$$

where \mathcal{A} and ω are the visibility amplitude and phase

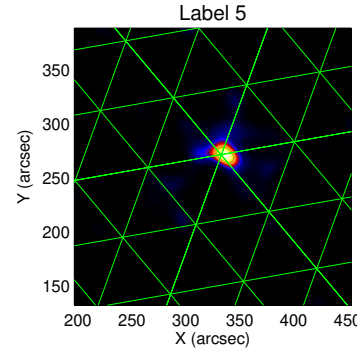
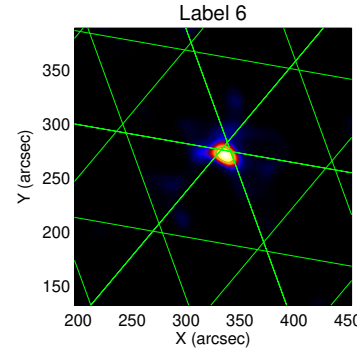
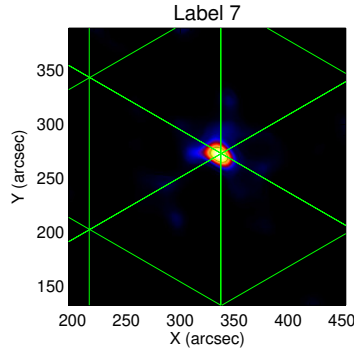
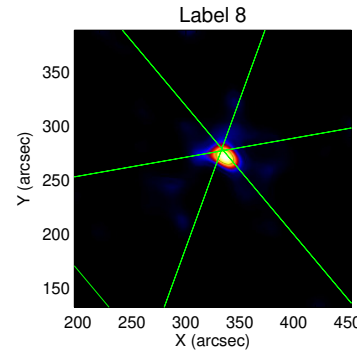
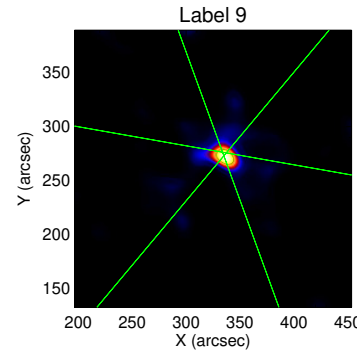
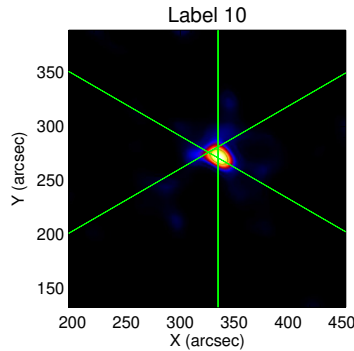
- We can associate to each visibility the set of lines corresponding to the maximum of the back-projection, i.e.,

$$2\pi(xu + yv) - \omega = 2\pi k, \quad k \in \mathbb{Z}$$



Back-projection lines

The back-projections lines corresponding to a compact X-ray source pass through the center of the source



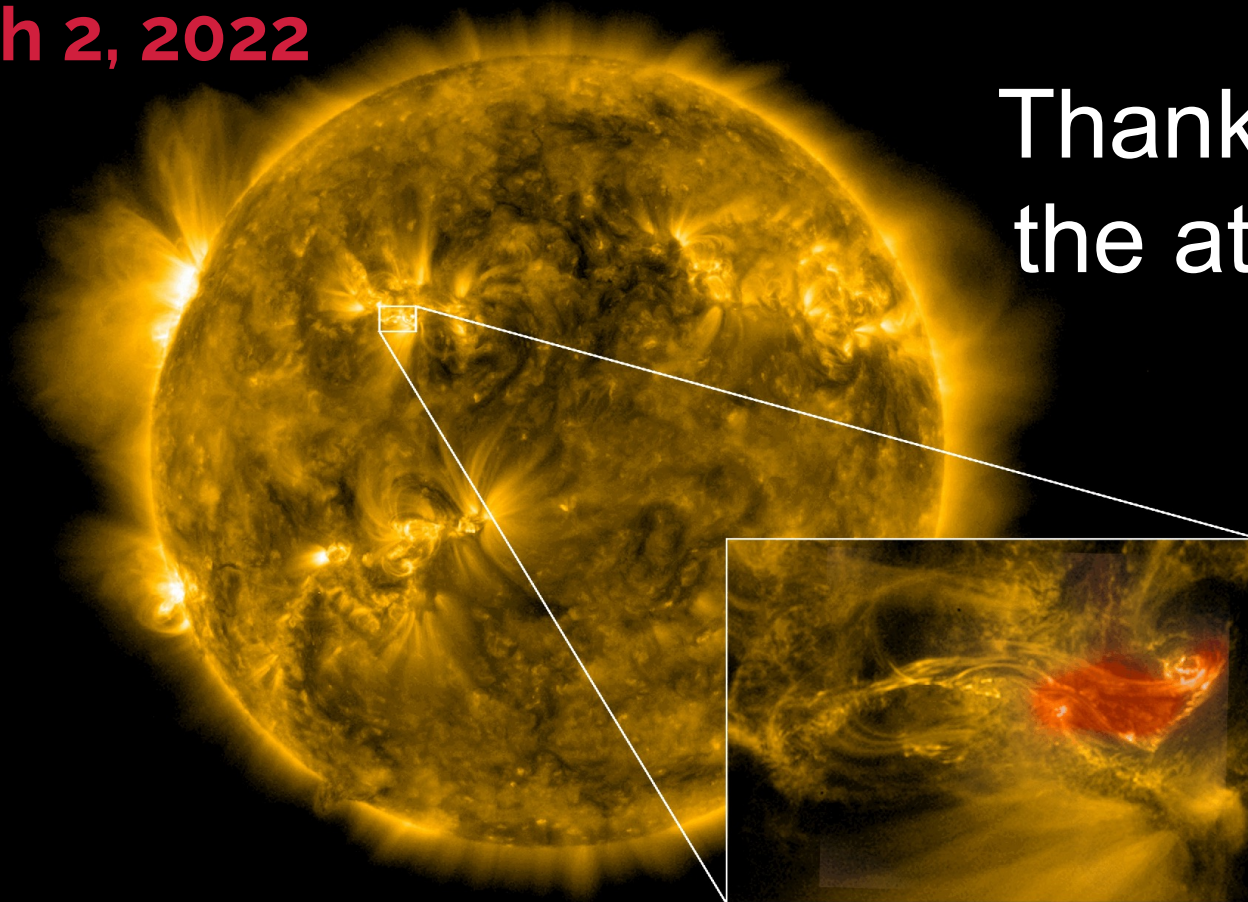
Conclusions

- We described the STIX imaging concept and the image reconstruction problem from STIX data
- We presented the MEM_GE method and we showed the results provided by this method when applied to experimental STIX data
- We provided an overview of the techniques we used for data calibration

References

- Battaglia et al., *STIX X-ray microflare observations during the Solar Orbiter commissioning phase*, A&A, 2021
- Högbom, *Aperture synthesis with a non-regular distribution of interferometer baselines*, Astronomy and Astrophysics Supplement, 1974
- Hurford et al, *The RHESSI imaging concept*, Solar Physics, 2002
- Krucker et al., *The Spectrometer/Telescope for Imaging X-rays (STIX)*, A&A, 2020
- Lin et al. , *The Reuven Ramaty High-Energy Solar Spectroscopic Imager (RHESSI)*, Solar Physics, 2002
- Massa et al., *Count-based imaging model for the Spectrometer/Telescope for Imaging X-rays (STIX) in Solar Orbiter*, A&A, 2019
- Massa et al., *MEM_GE: A New Maximum Entropy Method for Image Reconstruction from Solar X-Ray Visibilities*, APJ, 2020
- Massa et al., *Imaging from STIX visibility amplitudes*, A&A, 2021
- Massa et al., *First hard X-ray imaging results by Solar Orbiter STIX*, accepted for publication in Solar Physics, 2022
- Mertz et al., *Rotational aperture synthesis for x rays*, JOSA A, 1986
- Meuris et al., *Caliste-SO, a CdTe based spectrometer for bright solar event observations in hard X-rays*, Nucl. Instrum. Methods Phys. Res. A, 2015

March 2, 2022



Andrea Battaglia,
FHNW/ETH

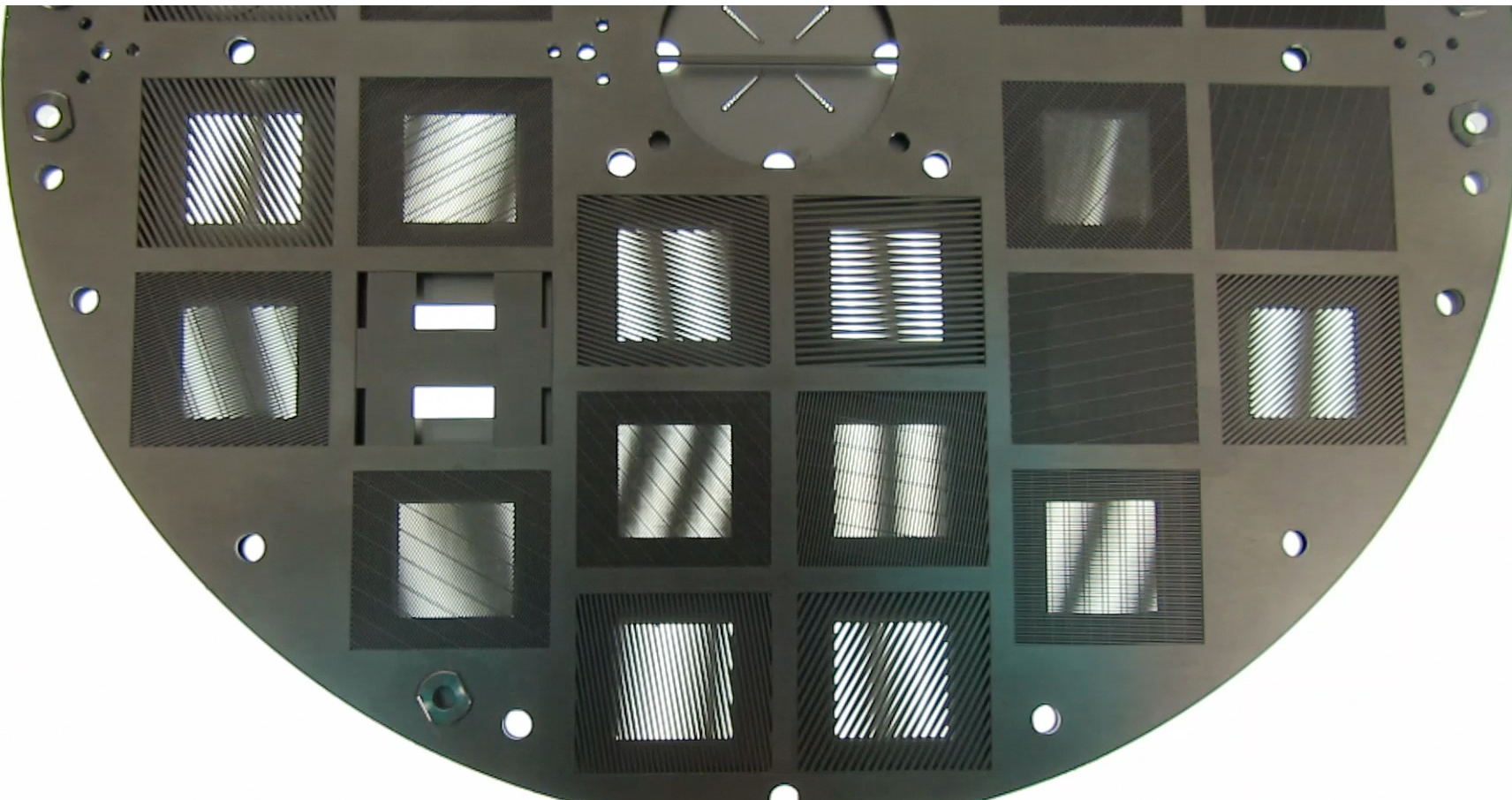
EUI/FSI 174 Å

EUI/HRI 174 Å
STIX 5-9 keV
STIX 16-50 keV

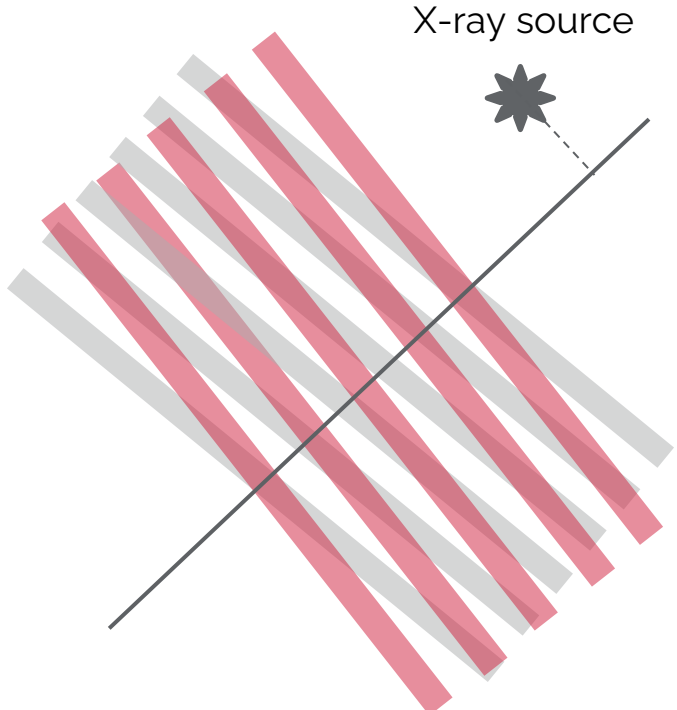
Thank you for
the attention!

The STIX imaging concept

The STIX imaging concept



The STIX imaging concept



Moiré patterns in a nutshell:

- sensitive to specific directions (grids' orientation, phase)
- sensitive to specific source sizes (grids' pitch, amplitude)

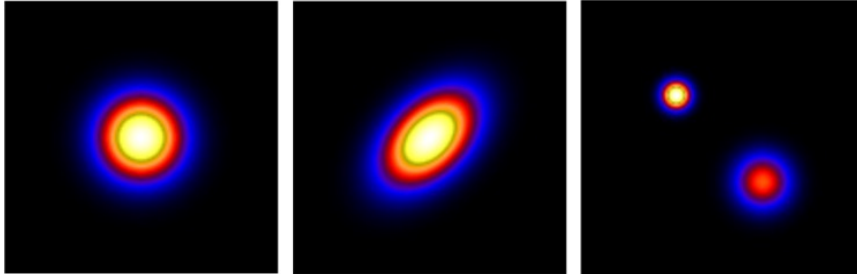
Each pattern contains information on a bi-dimensional Fourier component (**visibility**) of the hard X-ray flaring source

Imaging methods

Amplitude imaging

(Massa et al., 2021)

Choose a parametric shape ϕ_θ among



and solve

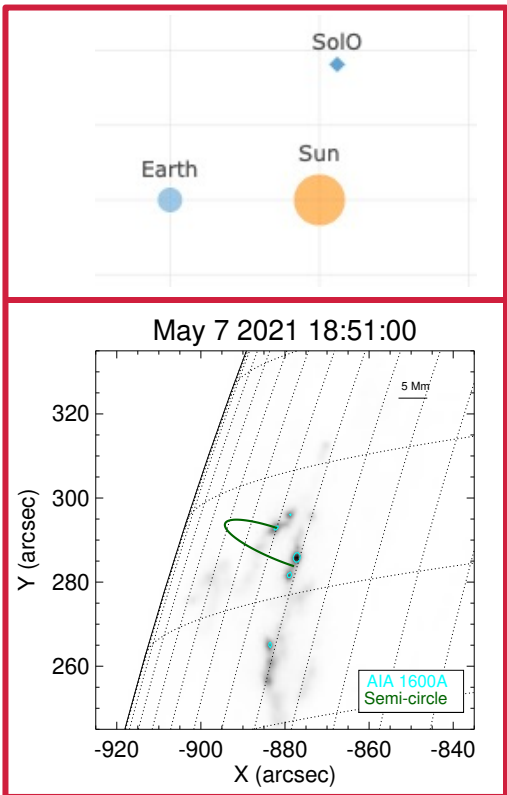
$$\theta^* = \operatorname{argmin}_\theta \sum_i \frac{|(F\phi_\theta)_i| - |V_i|)^2}{\sigma_i^2}$$

- First attempt to image reconstruction from STIX data
- Solve: $|F\phi| = |V|$
- Visibility amplitudes
 - Contain information on the source dimension and morphology
 - Do not contain information on the source location
- Parametric approach

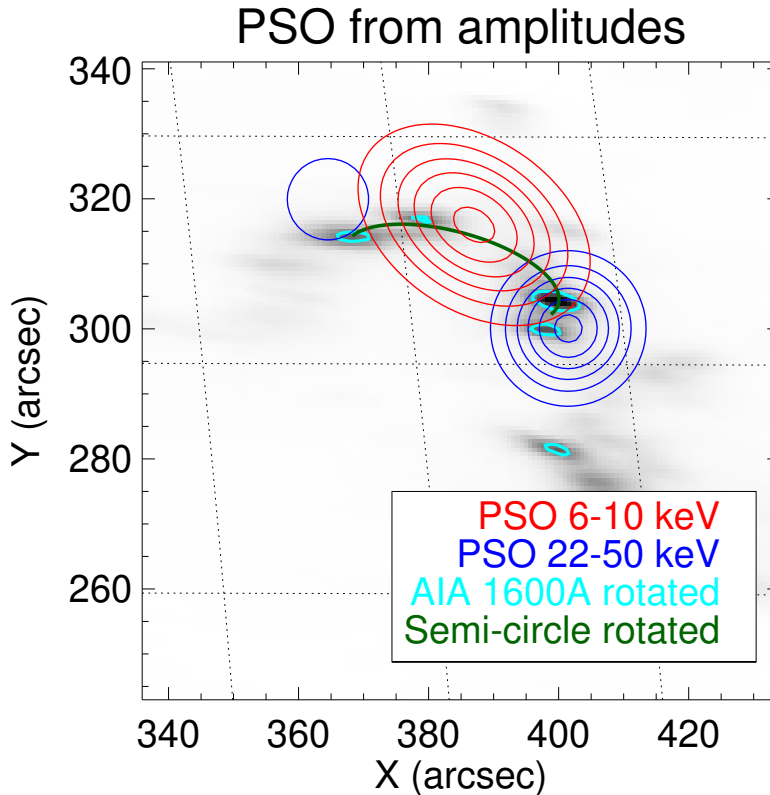
—

Amplitude imaging (Massa et al., 2021)

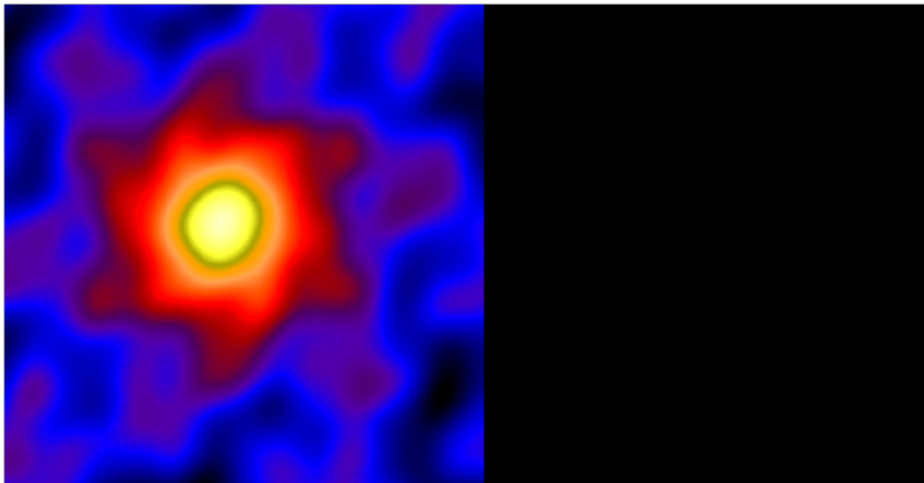
May 7 2021 event



Reprojected
AIA map
(see Battaglia et
al, 2021)



Clean

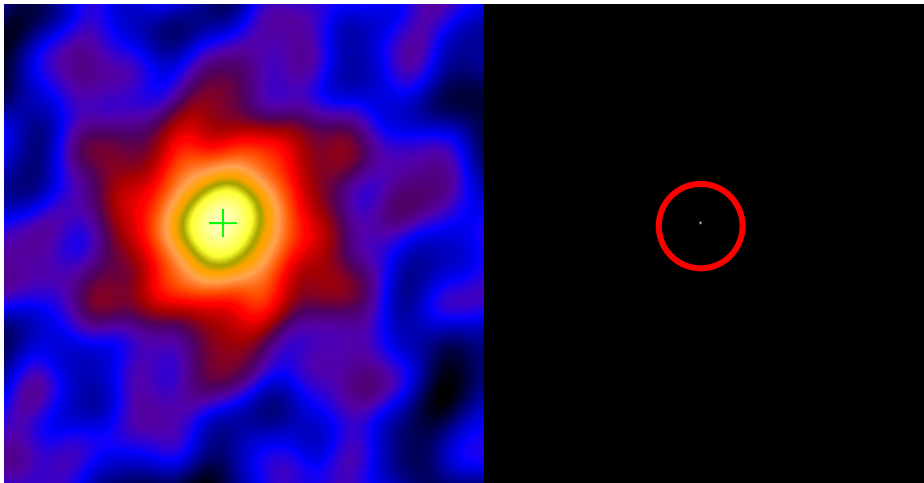


Iterative method:

- Creates two maps: **dirty map** (back projection) and **clean components (cc) map** (zero map)



Clean

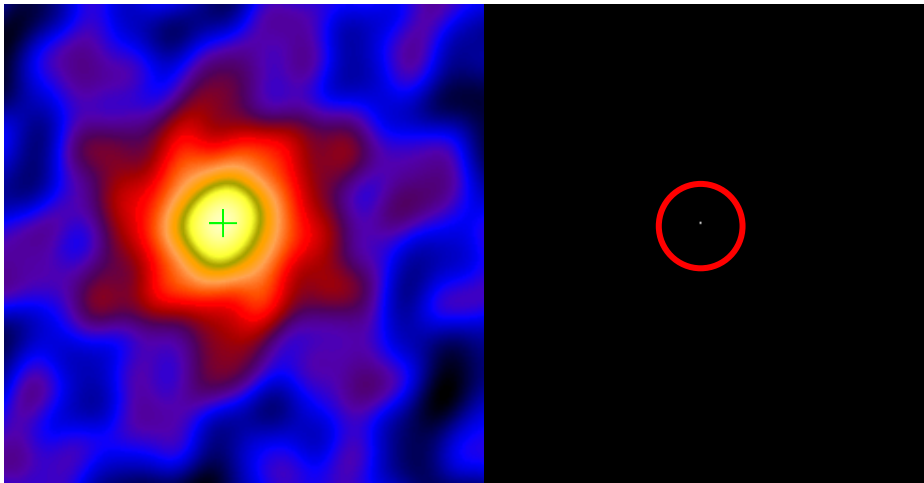


Iterative method:

- Creates two maps: **dirty map** (back projection) and **clean components (cc) map** (zero map)
- Finds maximum of the dirty map and add clean component in the cc map

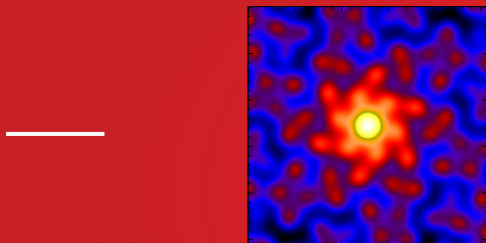


Clean



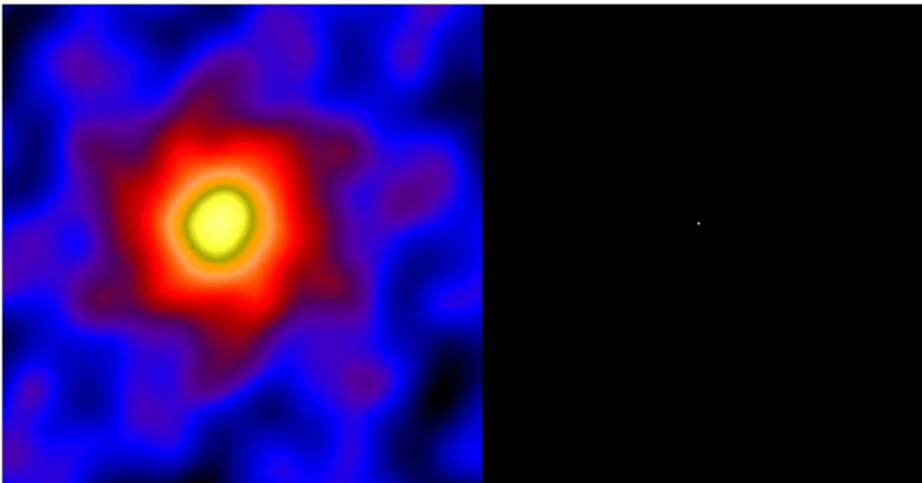
Iterative method:

- Creates two maps: **dirty map** (back projection) and **clean components (cc) map** (zero map)
- Finds maximum of the dirty map and add clean component in the cc map
- Subtracts a fraction of the PSF from the dirty map



WKU®

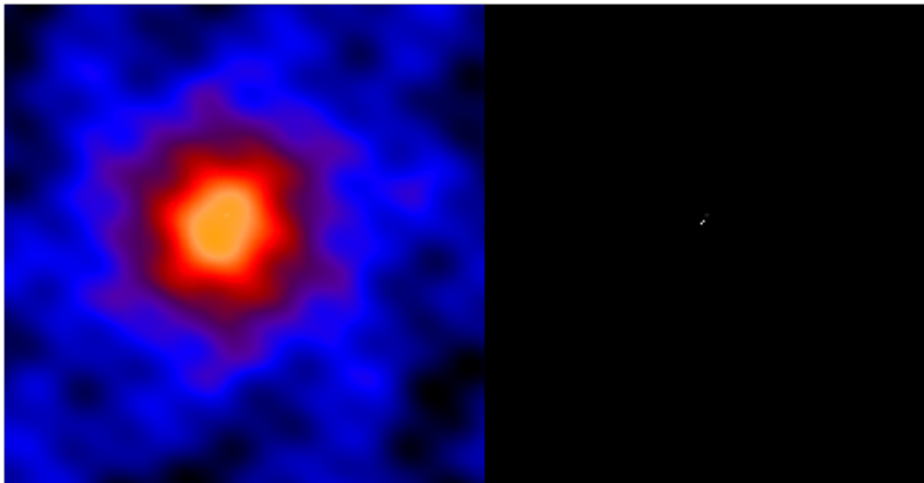
Clean



Iterative method:

- Creates two maps: **dirty map** (back projection) and **clean components (cc) map** (zero map)
- Finds maximum of the dirty map and add clean component in the cc map
- Subtracts a fraction of the PSF from the dirty map
- Iterates

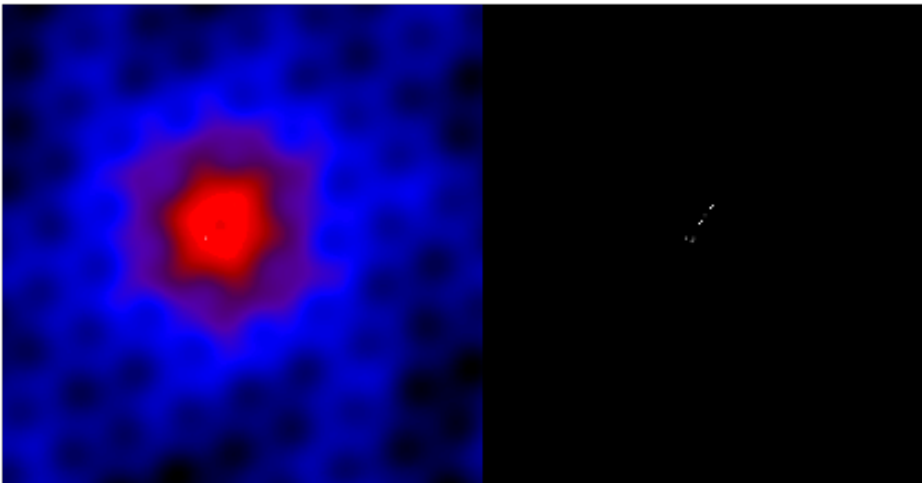
Clean



Iterative method:

- Creates two maps: **dirty map** (back projection) and **clean components (cc) map** (zero map)
- Finds maximum of the dirty map and add clean component in the cc map
- Subtracts a fraction of the PSF from the dirty map
- Iterates

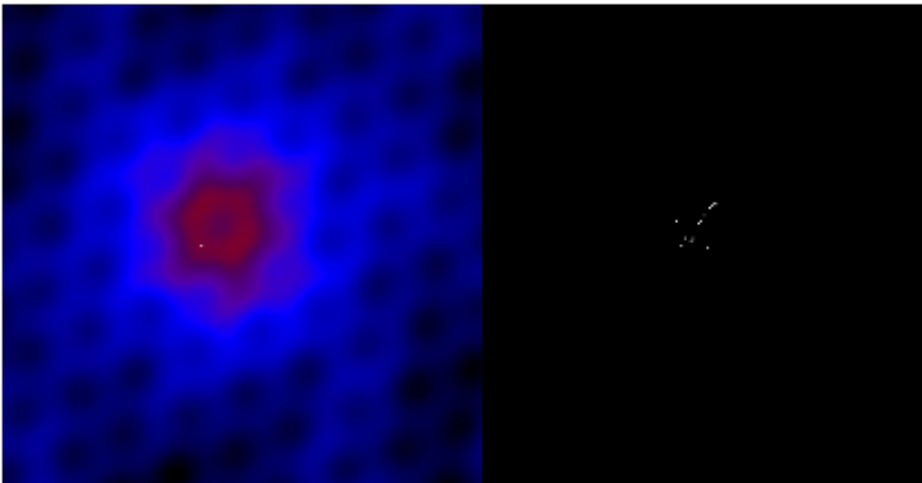
Clean



Iterative method:

- Creates two maps: **dirty map** (back projection) and **clean components (cc) map** (zero map)
- Finds maximum of the dirty map and add clean component in the cc map
- Subtracts a fraction of the PSF from the dirty map
- Iterates

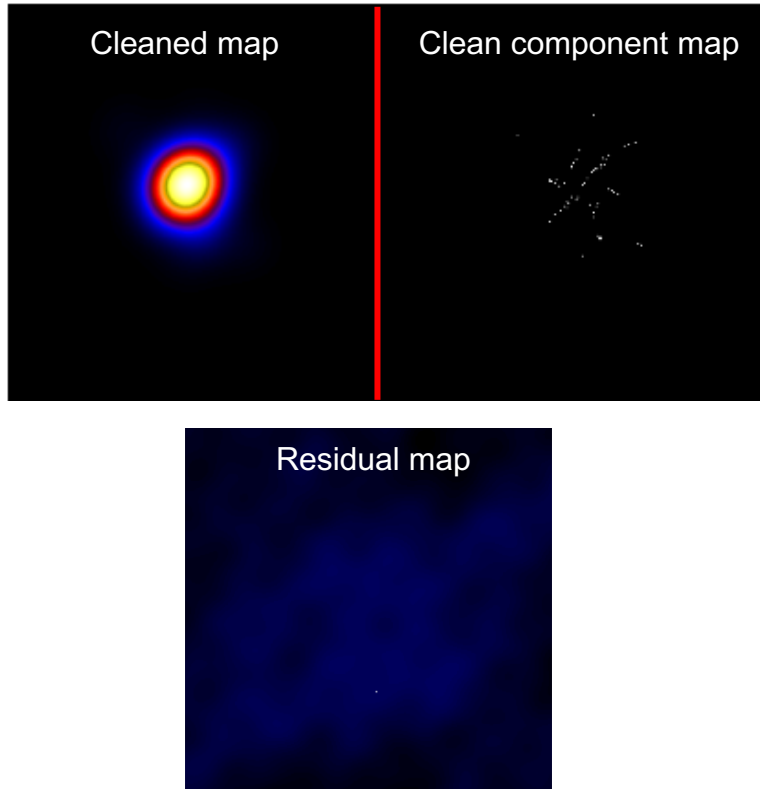
Clean



Iterative method:

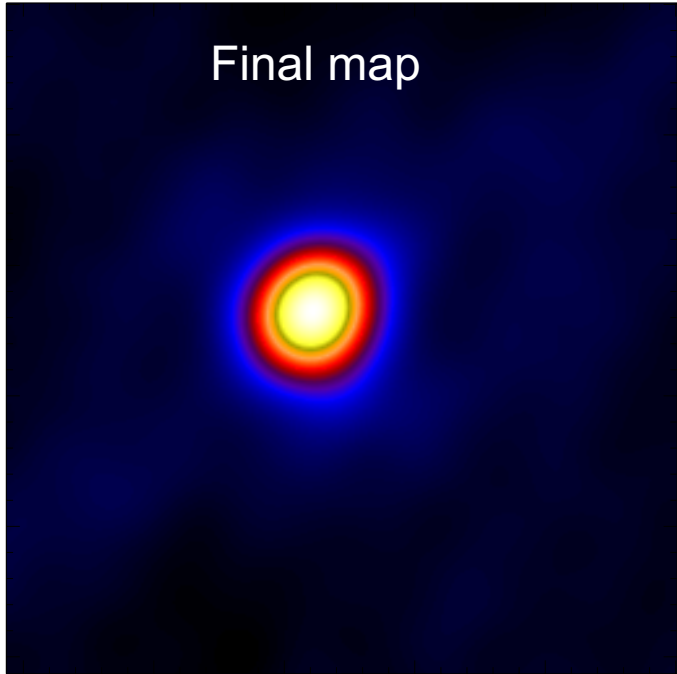
- Creates two maps: **dirty map** (back projection) and **clean components (cc) map** (zero map)
- Finds maximum of the dirty map and add clean component in the cc map
- Subtracts a fraction of the PSF from the dirty map
- Iterates

Clean



Final step: convolution with
clean beam and residuals

Clean

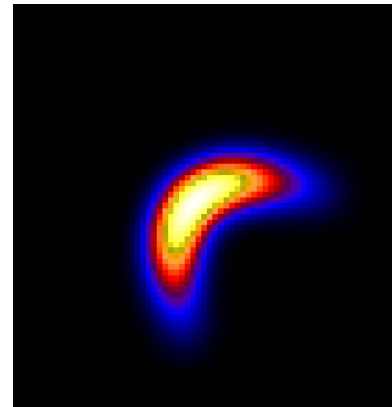
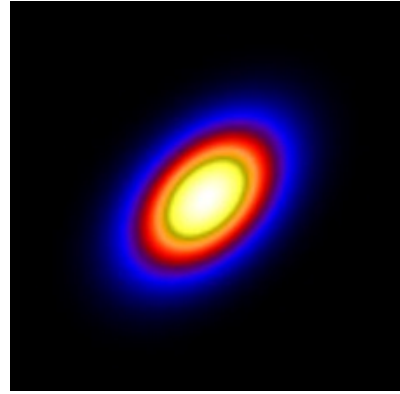
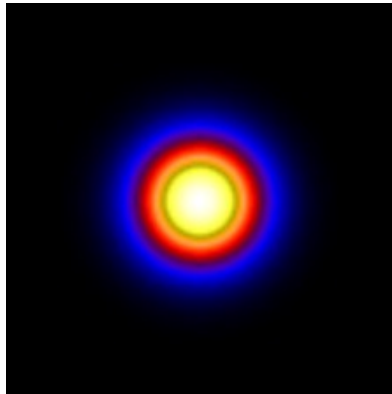


Final step: convolution with
clean beam and residuals



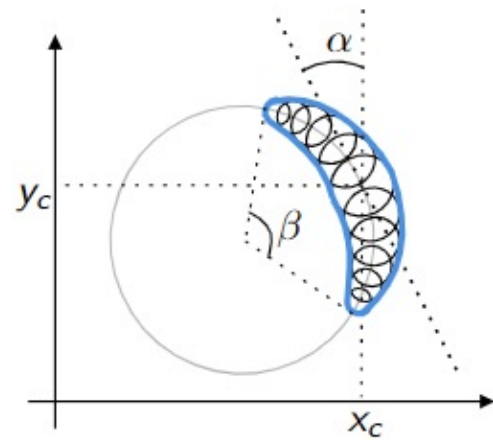
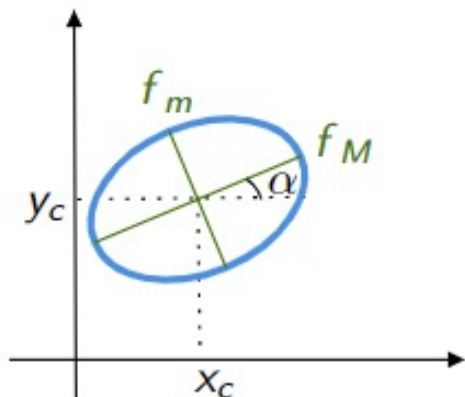
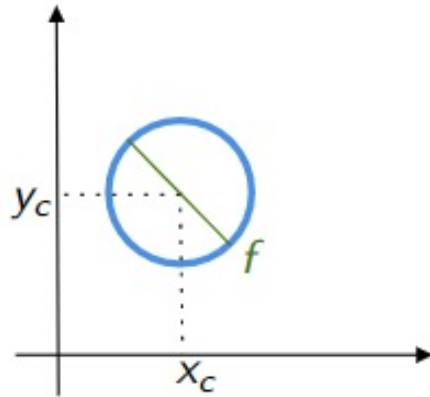
VIS_FWDFIT_PSO (Volpara et al., 2022)

- Parametric imaging
- Choose a parametric shape ϕ_θ among



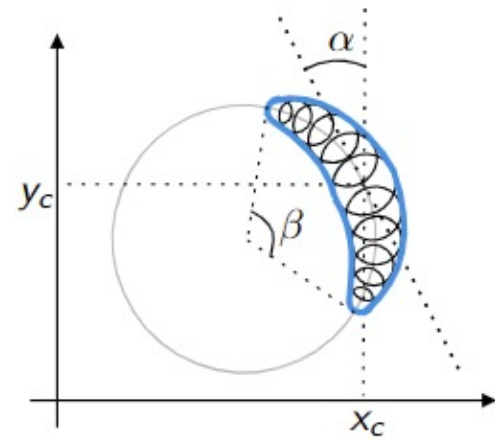
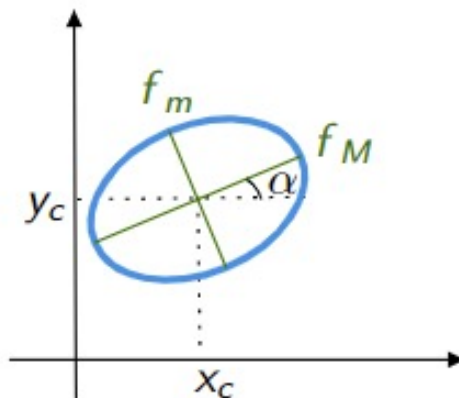
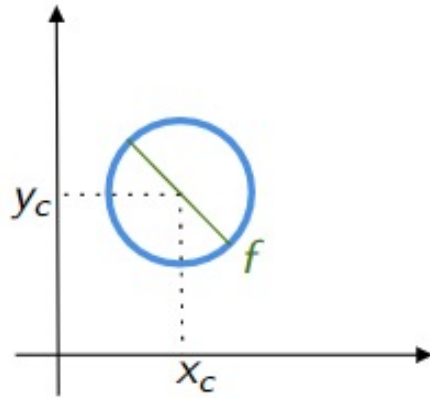
VIS_FWDFIT_PSO (Volpara et al., 2022)

- Parametric imaging
- Choose a parametric shape ϕ_θ among



VIS_FWDFIT_PSO (Volpara et al., 2022)

- Parametric imaging
- Choose a parametric shape ϕ_θ among

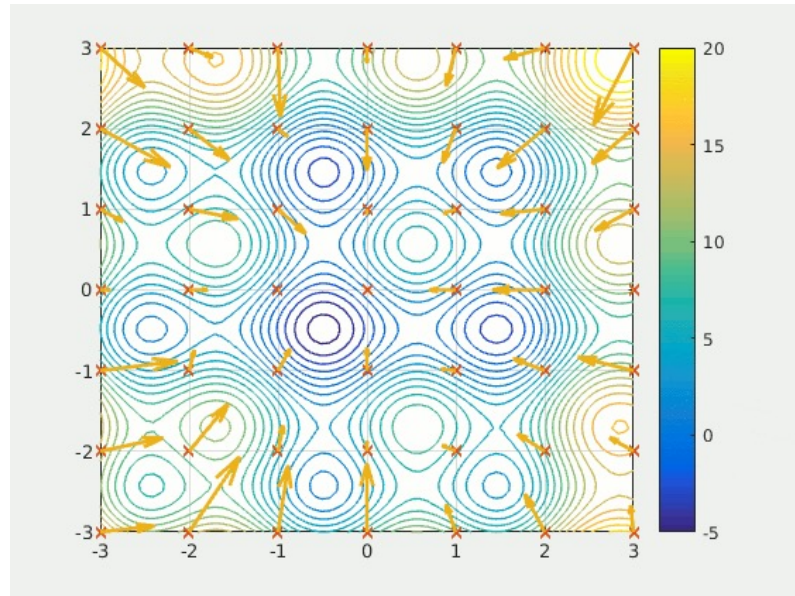


- Solve

$$\theta^* = \operatorname{argmin}_\theta \frac{1}{N_V - N_{\phi_\theta}} \sum_i \frac{|(F\phi_\theta)_i - V_i|^2}{\sigma_i^2}$$

VIS_FWDFIT_PSO (Volpara et al., 2022)

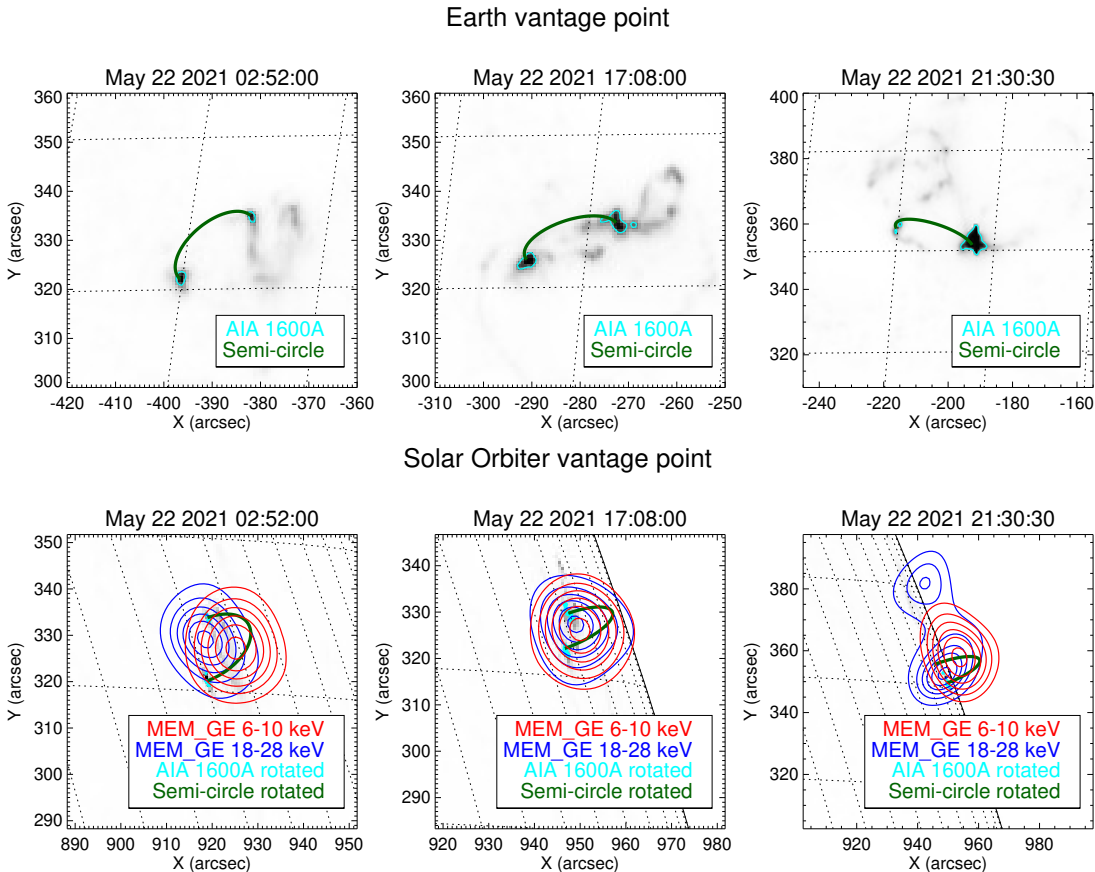
- **Uncertainty on the parameters:** 20 reconstructions from visibilities perturbed with Gaussian noise and computation of the standard deviation
- **New optimization method:** based on Particle Swarm Optimization (PSO, Eberhart et al., 1995)



By Ephramac - Own work, CC BY-SA 4.0,
<https://commons.wikimedia.org/w/index.php?curid=54975083>

Results

First imaging results (Massa et al., 2022)



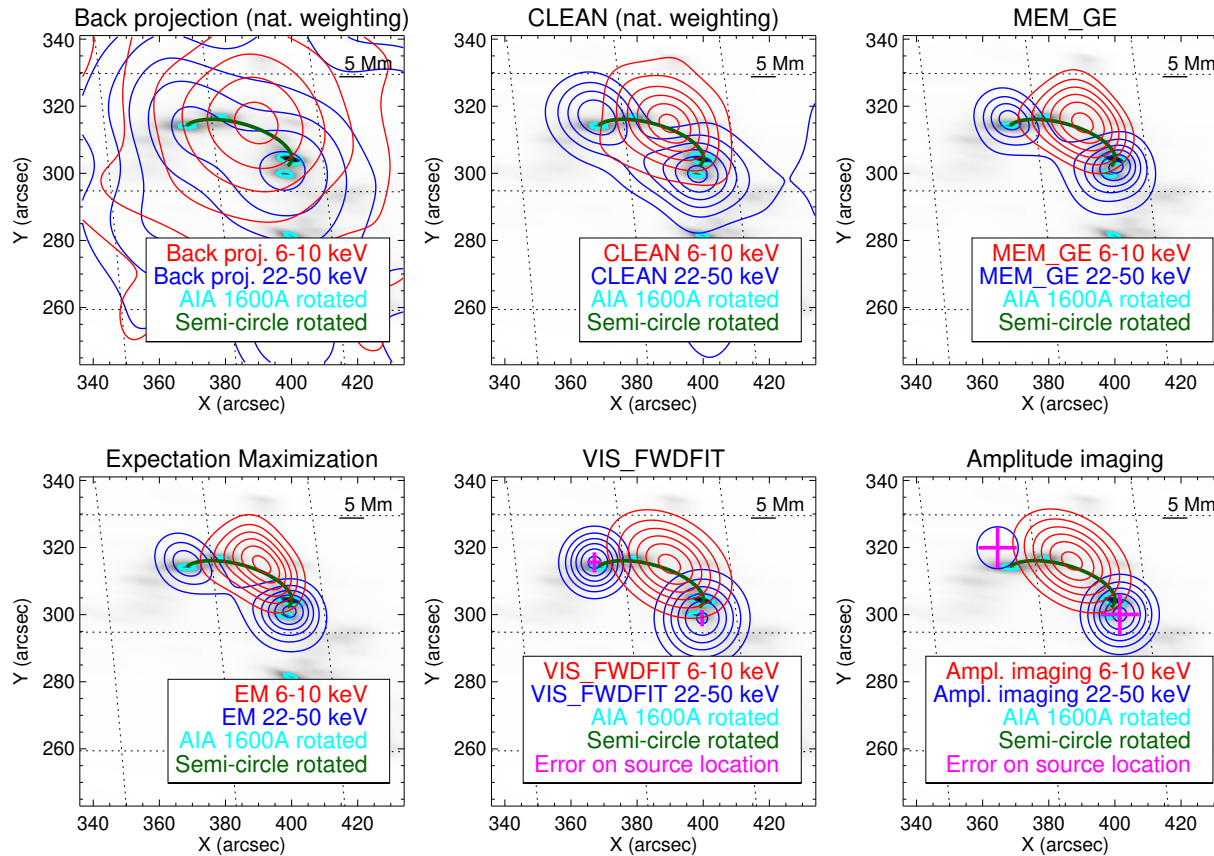
Active region AR2824

- 02:52:00 UT: GOES C6.1
- 17:08:00 UT: GOES M1.1
- 21:30:30 UT: GOES M1.4

Manual shift STIX reconstructions

Event	Δx (arcsec)	Δy (arcsec)
02:52	47	55
17:08	47	50
21:30	50	50

First imaging results (Massa et al., 2022)

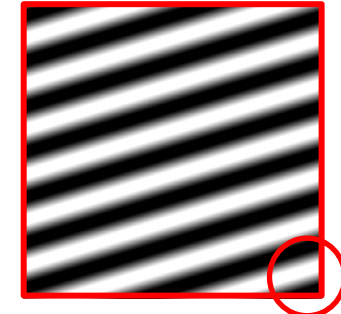
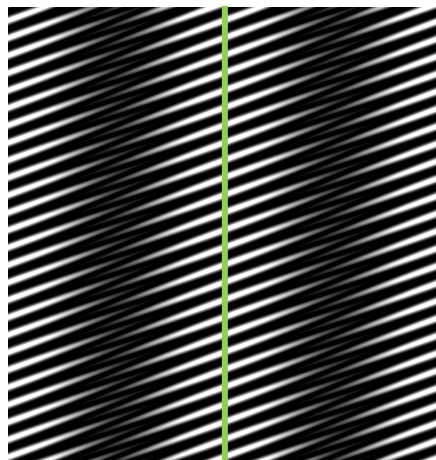


Data calibration

Visibility phase calibration

- Determine the correction factor ϕ_{calib} in $\phi = \text{atan}\left(\frac{D-B}{C-A}\right) + 45^\circ + \phi_{\text{calib}}$
- Check for potential instrument deformations

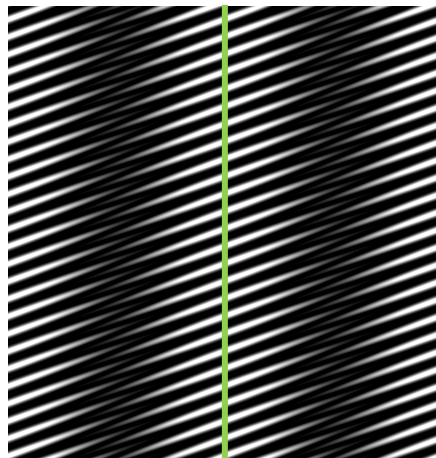
ϕ_{calib} is determined by the relative position of front and rear grid



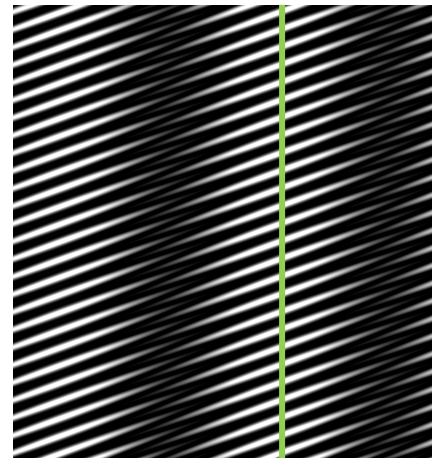
Visibility phase calibration

- Determine the correction factor ϕ_{calib} in $\phi = \tan\left(\frac{D-B}{C-A}\right) + 45^\circ + \phi_{\text{calib}}$
- Check for potential instrument deformations

ϕ_{calib} is determined by the relative position of front and rear grid



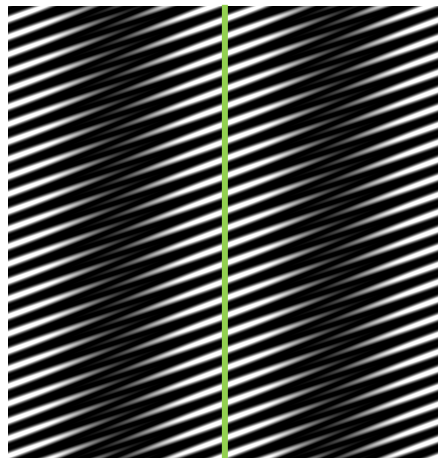
Shift front
grid →



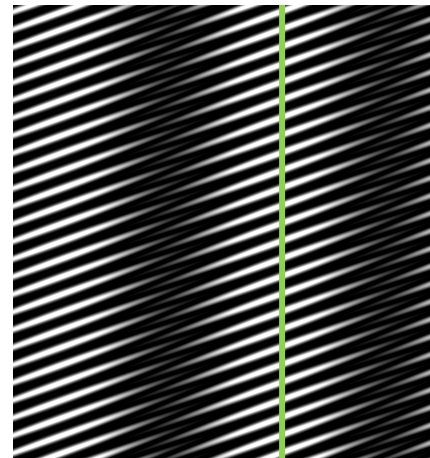
Visibility phase calibration

- Determine the correction factor ϕ_{calib} in $\phi = \tan\left(\frac{D-B}{C-A}\right) + 45^\circ + \phi_{\text{calib}}$
- Check for potential instrument deformations

ϕ_{calib} is determined by the relative position of front and rear grid

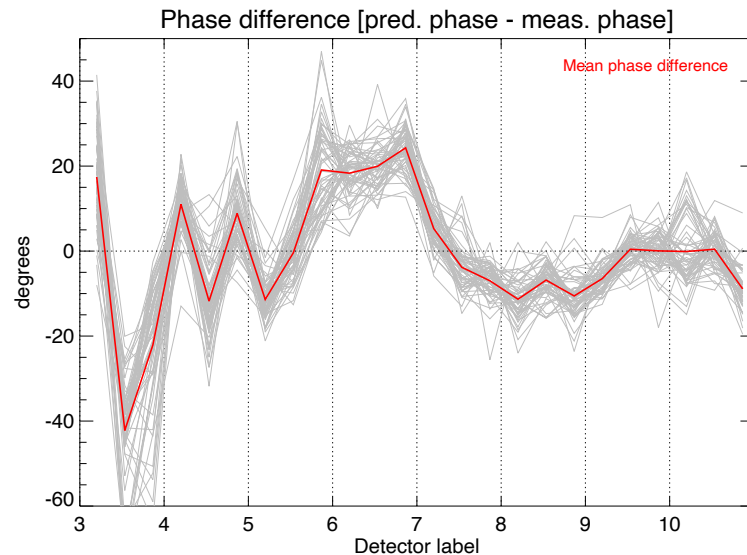


Shift front
grid →



Self calibration for visibility phases

- We considered a dataset of compact events, and we applied a forward fitting method (using a circular Gaussian shape)
- We computed the difference between the observed visibility phases and those predicted from the forward fitted source



Distortion factors

